

Rapporti tecnici INGV

**Battery control system for
remote stations**

220



Direttore

Enzo Boschi

Editorial Board

Raffaele Azzaro (CT)

Sara Barsotti (PI)

Mario Castellano (NA)

Viviana Castelli (BO)

Rosa Anna Corsaro (CT)

Luigi Cucci (RM1)

Mauro Di Vito (NA)

Marcello Liotta (PA)

Simona Masina (BO)

Mario Mattia (CT)

Nicola Pagliuca (RM1)

Umberto Sciacca (RM1)

Salvatore Stramondo (CNT)

Andrea Tertulliani - Editor in Chief (RM1)

Aldo Winkler (RM2)

Gaetano Zonno (MI)

Segreteria di Redazione

Francesca Di Stefano - coordinatore

Tel. +39 06 51860068

Fax +39 06 36915617

Rossella Celi

Tel. +39 06 51860055

Fax +39 06 36915617

redazionecen@ingv.it



Rapporti tecnici INGV

BATTERY CONTROL SYSTEM FOR REMOTE STATIONS

Manuele Di Persio, Cesidio Gizzi

INGV (Istituto Nazionale di Geofisica e Vulcanologia, Sezione Geomagnetismo, Aeronomia e Geofisica Ambientale)

220

Index

Introduction	5
1. Simple battery control whit diodes	5
2. Block diagram and circuit of the instrument	5
3. Analysis of the noise	9
4. Acquisition test	10
5. Conclusions	13

Introduction

Remote stations are located away from populated areas; as a consequence they need complementary power systems to avoid the lack of 220 V power line, such as photovoltaic panels coupled to 12 V batteries. However, the batteries suffer the repeated charge cycles that can reduce their lifetime. It is also difficult to test the state of the batteries during the day, because they are simultaneously charged by photovoltaic solar panels; if the batteries have problems, the stations may stop working during the night.

1. Simple battery control with diodes

Usually, remote stations are equipped with several batteries in parallel configuration. When a battery is damaged it corrupts the all the and to avoid this problem we can use the simple circuit of diodes as shown in Figure 1.

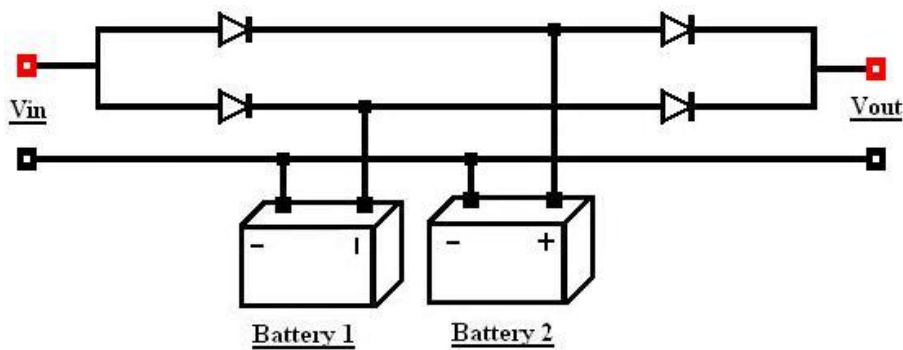


Figure 1. Possible solution.

It is possible to avoid the breakdown of the instrumentation using this circuit, but, however, there is no direct control of the system and it is not possible to know which battery is damaged because both batteries are continuously recharged; in addition, we have a voltage drop on diodes that increases with the current consumption. So, the output voltage is not equal to the voltage of the battery and magnetometers or other electronics are not properly powered. A device which uses operational amplifiers and discrete components has been projected to solve these problems.

2. Block diagram and circuit of the new device

This device, whose block diagram is shown in Figure 2, has three input and three output lines. The case of the instrument is made by aluminum, copper and brass, which are not ferromagnetic and they therefore do not disturb the magnetic measurements. The system is cooled by an automatic fan with hysteresis, ranging from 35°C to 50°C. The input 1 is connected to the photovoltaic panels regulator. The input 2 is connected to the main battery. The input 3 is connected to the secondary battery. Output A is the first output and it is regulated at about 13,5V / 2,5A. Output B is the second output and it is regulated at about 13,5V / 2,5A. The two outputs may be used to supply two different stations which are equipped with overhauser magnetometer, fluxgate magnetometer, GPS and communication boards. The output C is an unregulated voltage output which provides the voltage of the battery in use; the voltage range of this output is from 11 V to 14 V with the same current that comes directly from the battery. The ground lines of the three outputs are separated, but the ground lines of output A and output B may be combined while the ground of output C must remain separated.

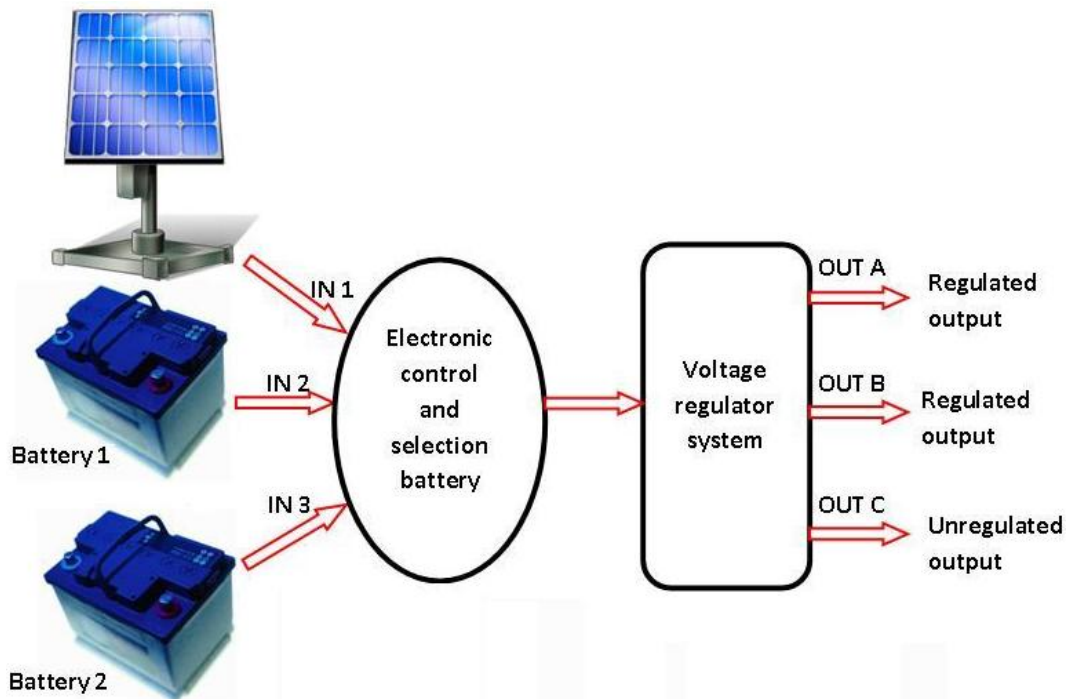


Figure 2. Block diagram of the instruments.

Both the batteries are in charging mode, but only battery 1 is connected to the system. If this battery loses efficiency and during the night its voltage decreases, the control unit disconnects the battery 1 and connects the second battery. This exchange occurs without voltage drops on the output, so that the powered magnetometers do not switch off. On the front side of the case there are two LEDs (red and green) and a push switch for setting up the electronics. When the main battery is in use, the green LED is on; if the first battery is exchanged the green LED turns off and the red LED comes on. Switching occurs when the voltage of battery 1 is about 10.5 V, to avoid the damage of the battery; in this case it is possible to check if the battery 1 has problems and eventually to replace it or to reconnect it. Figures 3 and 4 show the electronic circuits of the battery control system. Table 1 and 2 are the lists of the electronic components used. The double operational amplifier U4A works as a comparator and it triggers the battery exchange; the RC network on transistor Q1 introduces the delay $\tau \approx 1\text{sec}$. The two operational amplifiers U4B and U5 drive the two relays at different times; the control of these relays is such that there is always one battery connected to the voltage regulator. The output relays can be replaced with solid state relays or other systems of switches. After connecting the batteries to the inputs the red LED is on and the battery 2 is in operation mode; to set up the device the push switch must be pressed until the red LED turns off and the green LED comes on; in this way, the battery 1 is operating and the system is active. The device is powered directly from the active battery; it absorbs about 400 mA when the fan is turned on and 250 mA when it is off. The power consumption without fan is due to the regulator output voltage.

The use of discrete electronic components and the simplicity of this implementation make this board versatile, and its configuration can be modified to adapt it to other contexts. For example, the output voltage can be modified or it is possible to control the battery exchange without adjusting the output voltage. In this case the consumption is reduced to about 100 mA. In figure 5 it is shown the case of the device, the position of the controls and of the input and output connectors.

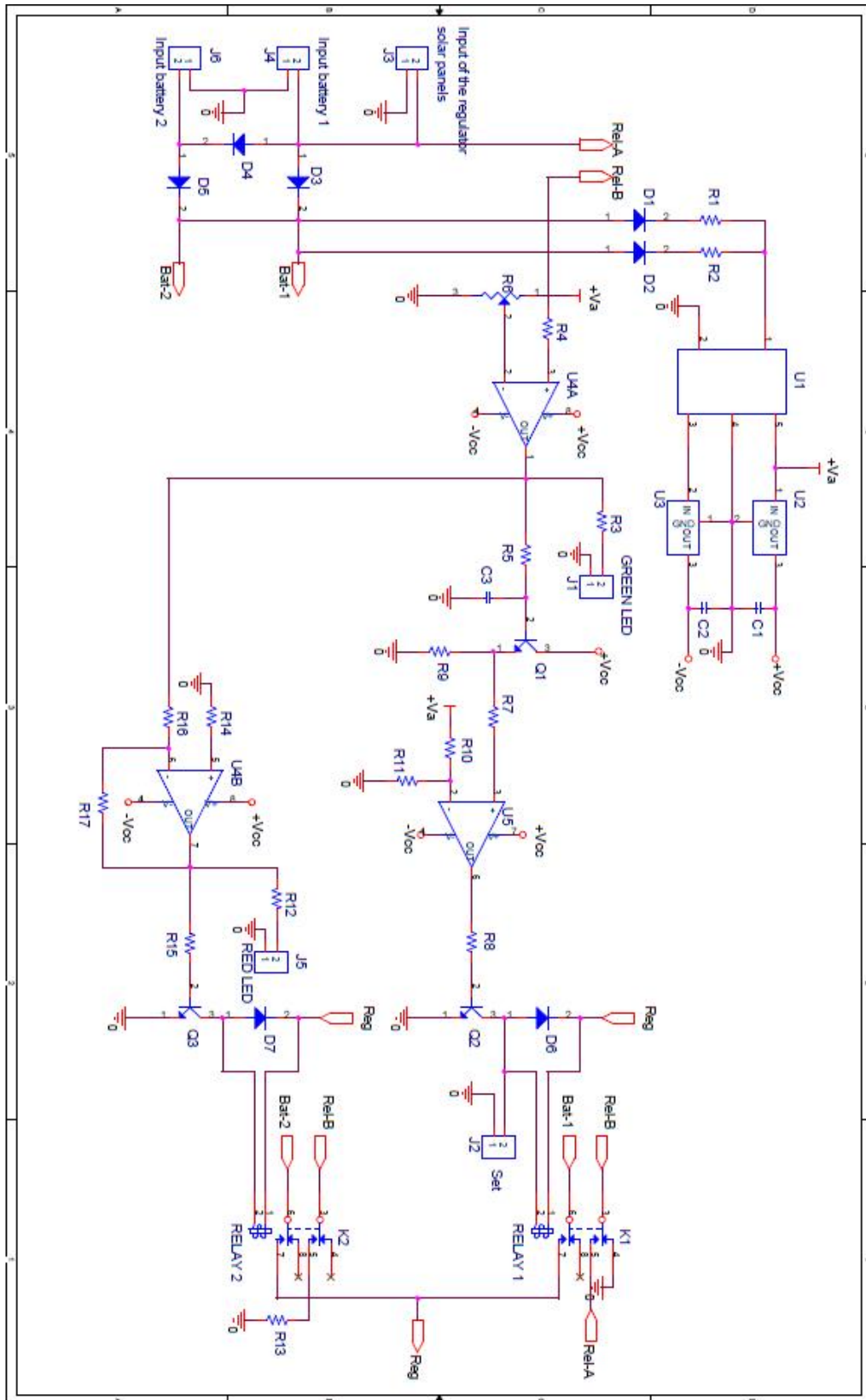


Figure 3. Circuit of the electronic control.

Reference part	Type	Value
R1, R2	Resistors	1 Ω
R3	Resistor	540 Ω
R4, R7, R9	Resistors	4.7 k Ω
R5, R14, R16, R17	Resistors	470 k Ω
R6	Resistor Var.	10 k Ω
R8, R15	Resistors	2.4 k Ω
R10	Resistor	10 k Ω
R11	Resistor	1.56 k Ω
R12	Resistor	540 Ω
R13	Resistor	10 Ω
D1, D2, D6, D7	Diode	1N4001
D3, D4, D5	Diode	P600M
Q1, Q2, Q3	Transistor	2N2222
U1	DC/DC	TEN5-1223
U2	Regulator	LM7812
U3	Regulator	LM7912
U4	Double OPA	TL072
U5	Single OPA	TL071
C1, C2	Capacitors	220nF / 100V
C3	Capacitor	2.2uF / 65V
K1, K2	Relay	12V / 16A

Table 1. Component list of the electronic control.

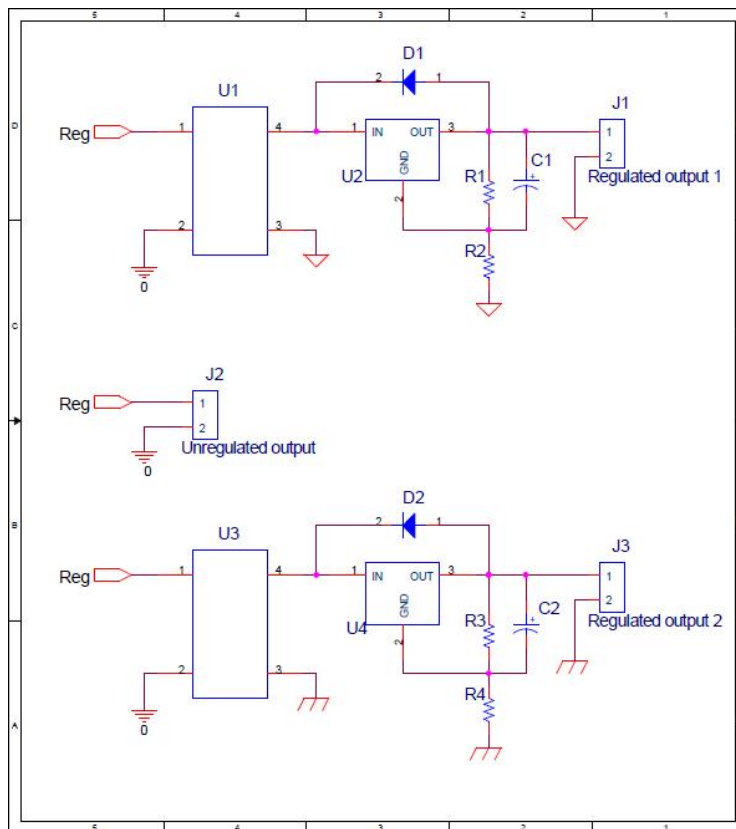


Figure 4. Circuit of the regulator voltage.

Reference part	Type	Value
R1, R3	Resistors	120 Ω
R2, R4	Resistors	1.2 k Ω
U1, U3	DC/DC	TEN40-2413
U2, U4	Regulator	LM338
D1, D2	Diode	1N4001
C1, C2	Capacitor	2.2 μ F / 65V

Table 2. Component list of the voltage regulator.

The resistors R1 and R2 have a thermal power of 2 W and the resistor R13 has a thermal power of 25 W; other resistors have a thermal power of 1/8 W; it is not necessary that the resistors have high precision. The simple ON-OFF operation of the system does not require high precision components and low noise operational amplifiers.

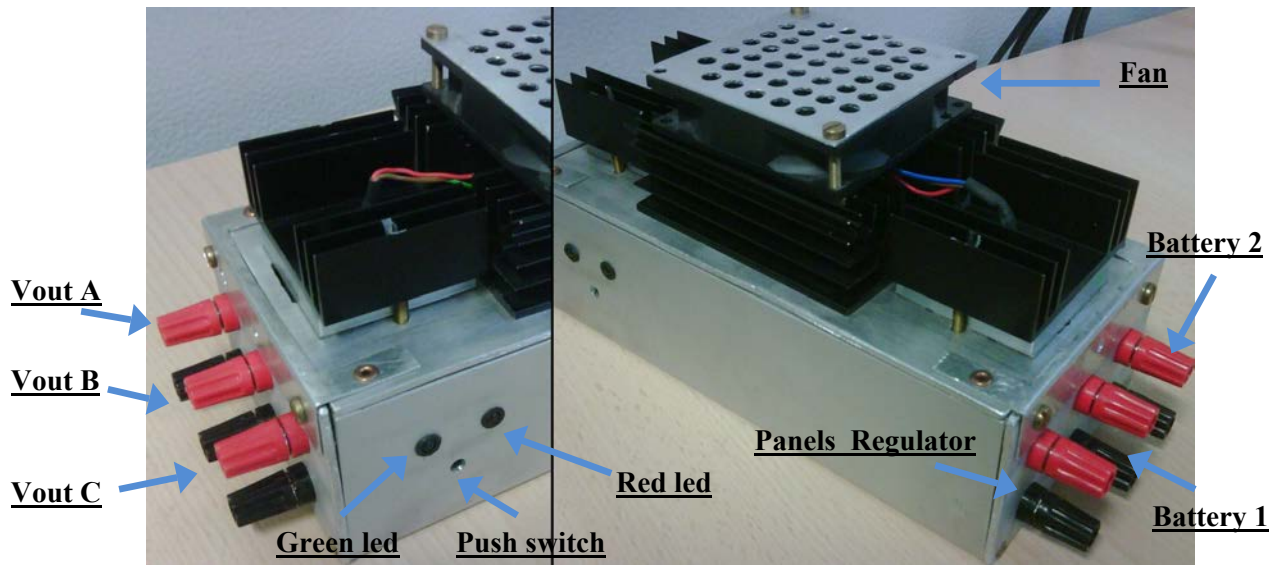


Figure 5. Input and output lines of the instrument.

3. Analysis of the noise

Input and output connectors are the only metallic components and their potential interference on the quality of magnetic data must be tested. In Table 3 static (fan “off”) and dynamic (fan “on”) influence on the data acquired by a single fluxgate sensor are shown. The interference was measured aligning the device with the axis of the fluxgate sensor; at a distance of 2 m the interference introduced by this device is negligible.

Distance (m)	Fan OFF (nT)	Fan ON (nT)
2	0	0
1	0	0,6
0,5	0,2	4
0,1	6	50

Table 3. Influence of the instrument on the data with fan off and fan on.

4. Acquisition test

We evaluated with two identical overhauser magnetometer if the device introduces any interference during the measurement of a magnetic field. The test was made with the magnetometer commonly used for the Intermagnet data acquisition (F1 values) and another (F2 values) placed in the geomagnetic absolute measurements building.

The term Intermagnet, (INTERNational Real-time MAGnetic Observatory NETWORK), indicates a worldwide network of magnetic observatories. The absolute measurements are the manual evaluation of the angles of inclination and declination of the geomagnetic field. The distance between the two magnetometers is approximately 30 m. We tested the interference introduced by the new device placing it at different distances from the second magnetometer, with the fan on and off and using the first as a reference magnetometer. We considered one minute of acquisition for each step with a 5 seconds sampling frequency. The sequence of the operations in this test was:

Distance 5 m fan ON for one minute and fan OFF for one minute.

Pause.

Distance 2 m fan ON for one minute and fan OFF for one minute.

Pause.

Distance 1 m fan ON for one minute and fan OFF for one minute.

The results obtained are shown in Tables 4, Table 5 and Table 6, where the ΔF was calculated as the difference between the two values F1 and F2.

Data at distance 5 m

Universal Time	F1(nT)	F2(nT)	ΔF (nT)
9:43:00	46462,6	46457,5	5,1
9:43:05	46462,6	46457,5	5,1
9:43:10	46462,6	46457,5	5,1
9:43:15	46462,6	46457,4	5,2
9:43:20	46462,5	46457,4	5,1
9:43:25	46462,6	46457,4	5,2
9:43:30	46462,6	46457,4	5,2
9:43:35	46462,6	46457,4	5,2
9:43:40	46462,6	46457,4	5,2
9:43:45	46462,6	46457,4	5,2
9:43:50	46462,5	46457,4	5,1
9:43:55	46462,5	46457,4	5,1
9:44:00	46462,5	46457,3	5,2
9:44:05	46462,6	46457,4	5,2
9:44:10	46462,6	46457,4	5,2
9:44:15	46462,6	46457,4	5,2
9:44:20	46462,5	46457,3	5,2
9:44:25	46462,5	46457,3	5,2
9:44:30	46462,5	46457,4	5,1
9:44:35	46462,5	46457,4	5,1
9:44:40	46462,5	46457,4	5,1
9:44:45	46462,5	46457,4	5,1
9:44:50	46462,5	46457,3	5,2
9:44:55	46462,5	46457,3	5,2

Table 4. First acquisition step.

Data at distance 2 m

Universal Time	F1(nT)	F2(nT)	ΔF (nT)
9:46:00	46462,6	46457,6	5
9:46:05	46462,7	46457,6	5,1
9:46:10	46462,7	46457,5	5,2
9:46:15	46462,7	46457,6	5,1
9:46:20	46462,7	46457,6	5,1
9:46:25	46462,7	46457,5	5,2
9:46:30	46462,7	46457,5	5,2
9:46:35	46462,7	46457,6	5,1
9:46:40	46462,7	46457,6	5,1
9:46:45	46462,7	46457,5	5,2
9:46:50	46462,7	46457,5	5,2
9:46:55	46462,7	46457,6	5,1
9:47:00	46462,7	46457,6	5,1
9:47:05	46462,7	46457,6	5,1
9:47:10	46462,7	46457,6	5,1
9:47:15	46462,7	46457,5	5,2
9:47:20	46462,7	46457,5	5,2
9:47:25	46462,7	46457,6	5,1
9:47:30	46462,7	46457,6	5,1
9:47:35	46462,7	46457,6	5,1
9:47:40	46462,7	46457,5	5,2
9:47:45	46462,7	46457,5	5,2
9:47:50	46462,7	46457,5	5,2
9:47:55	46462,7	46457,5	5,2

Table 5. Second acquisition step.

Data at distance 1 m

Universal Time	F1(nT)	F2(nT)	ΔF (nT)
9:49:00	46462,6	46457,8	4,8
9:49:05	46462,5	46457,9	4,6
9:49:10	46462,6	46458,1	4,5
9:49:15	46462,6	46458,1	4,5
9:49:20	46462,7	46458,1	4,6
9:49:25	46462,7	46458	4,7
9:49:30	46462,7	46457,9	4,8
9:49:35	46462,7	46457,8	4,9
9:49:40	46462,6	46457,8	4,8
9:49:45	46462,6	46457,8	4,8
9:49:50	46462,6	46457,9	4,7
9:49:55	46462,6	46457,9	4,7
9:50:00	46462,6	46457,8	4,8
9:50:05	46462,5	46458,2	4,3
9:50:10	46462,5	46458,2	4,3
9:50:15	46462,5	46458,1	4,4
9:50:20	46462,5	46458,1	4,4
9:50:25	46462,5	46458,1	4,4
9:50:30	46462,5	46458,2	4,3
9:50:35	46462,5	46458,2	4,3
9:50:40	46462,5	46458,1	4,4
9:50:45	46462,5	46458,2	4,3
9:50:50	46462,5	46458,2	4,3
9:50:55	46462,5	46458,1	4,4

Table 6. Third acquisition step.

In figures 6, 7 and 8 the ΔF values are shown in the three cases.

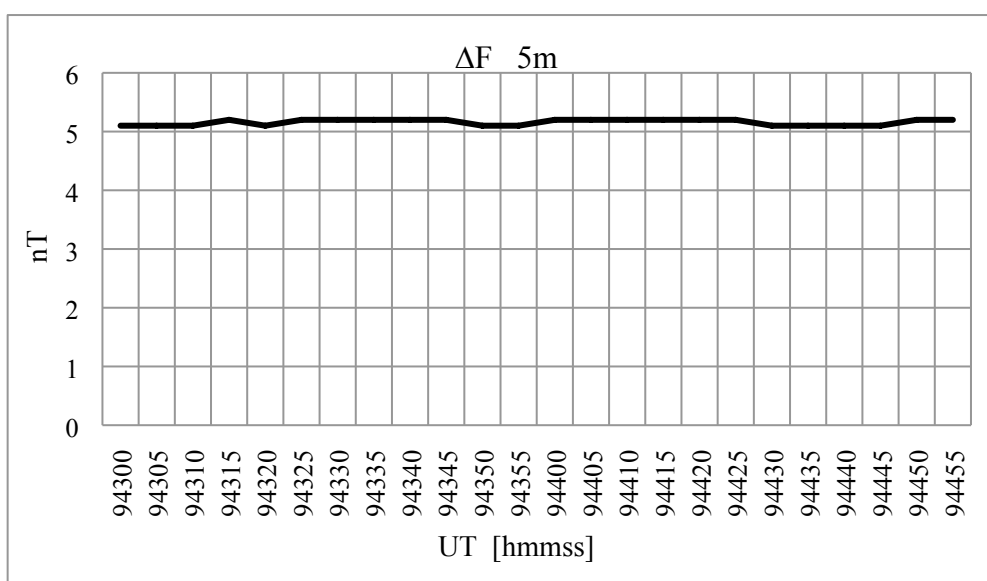


Figure 6. ΔF at 5 m.

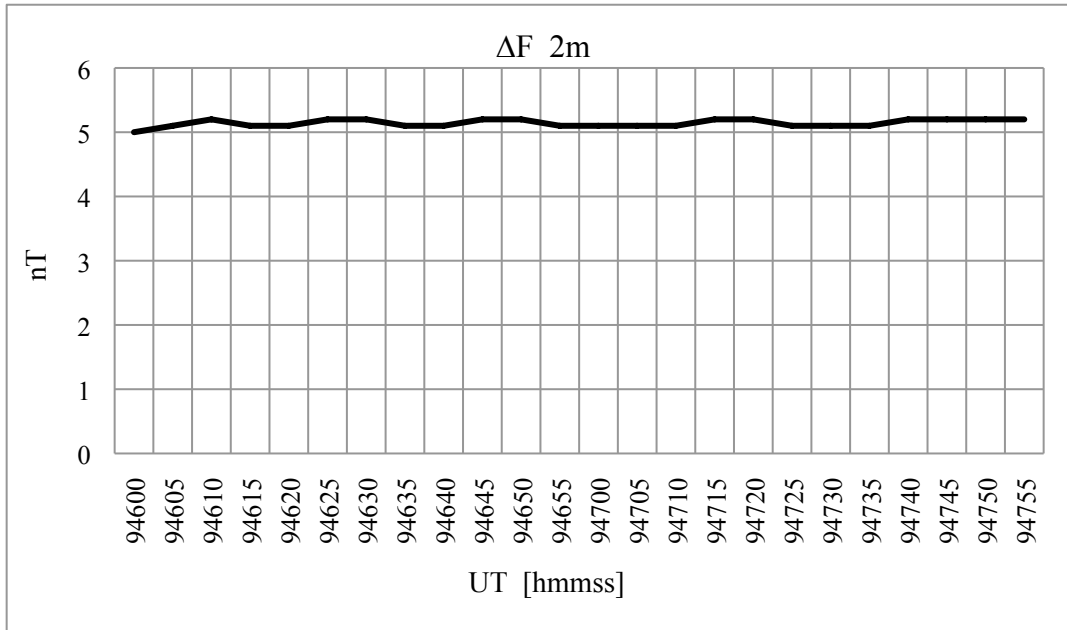


Figure 7. ΔF at 2 m.

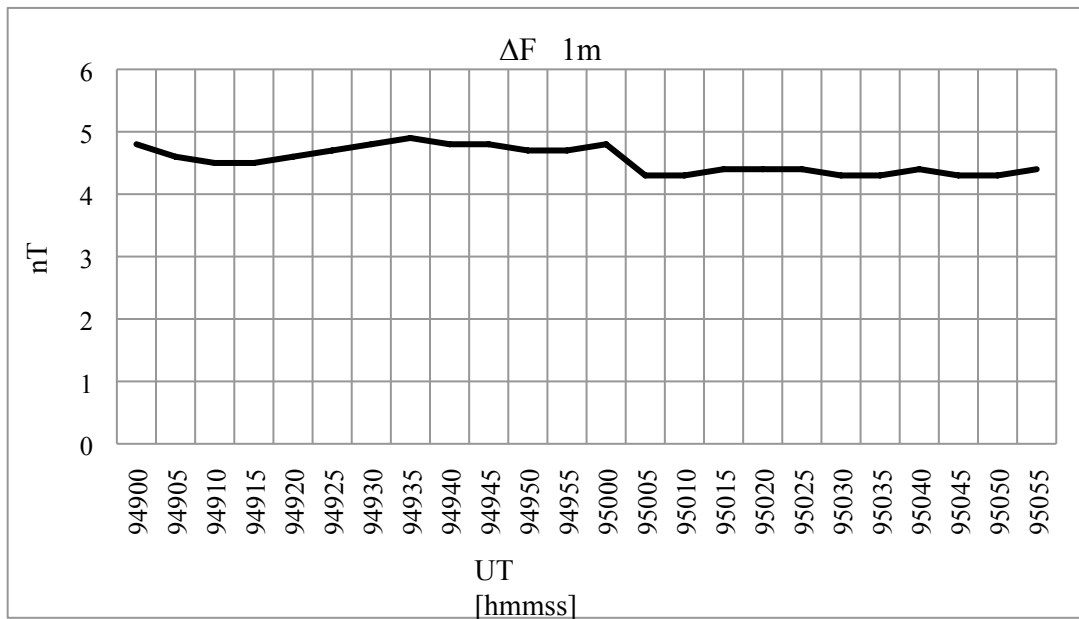


Figure 8. ΔF at 1 m.

Comparing the acquisitions at 5 m and 2 m we can see that ΔF remains practically unchanged. It means that the equipment does not introduce any interference for distances higher or equal to 2 m. For 1 m distance the ΔF decreased below 5 nT, so an interference is introduced by the device. In the third graph it is particularly evident a 0.5 nT step at the beginning of the minute in which we turned off the fan (UT 9:50:00).

5. Conclusions

This new board has been built for the geomagnetic observatory of Lampedusa and will be employed on the remote stations and observatories with criticities in the power supply. We tested the interference introduced by this device on standard magnetic field measurements and we concluded that at a distance higher than two meters it is negligible. Additional noise tests will be conducted analyzing its impact on geomagnetic data acquisition.

Coordinamento editoriale e impaginazione

Centro Editoriale Nazionale | INGV

Progetto grafico e redazionale

Daniela Riposati | Laboratorio Grafica e Immagini | INGV

© 2012 INGV Istituto Nazionale di Geofisica e Vulcanologia

Via di Vigna Murata, 605

00143 Roma

Tel. +39 06518601 Fax +39 065041181

<http://www.ingv.it>



Istituto Nazionale di Geofisica e Vulcanologia